ORIGINAL PAPER

Journal of Textile Engineering (2014), Vol.60, No.2, 27 – 34

Processing and Electrical Response of Fully Polymer Piezoelectric Filaments for E-Textiles Applications

Martins Rui [a], Silva Marco [b], Gonçalves Renato [b], Rocha Gerardo [c], Nóbrega J. Miguel [d], Carvalho Helder [a, *], Souto Pedro [a], Lanceros-Mendez Senentxu [b]

[a] *Centre for Textile Science and Technology, University of Minho, Guimarães, Portugal, University of Minho, Guimarães, Portugal*
[b] *Centre/Department of Physics, University of Minho, Guimarães, Portugal*
[c] *Dep. Industrial Electronics, University of Minho, Guimarães, Portugal*
[d] *IPC/I3N – Institute for Polymers and Composites*

Received 7 January 2013, accepted for publication 12 September 2013

Abstract

This paper describes the production and characterization of novel geometries for piezoelectric products with a large potential in the design and implementation of flexible sensors produced at low cost and high rates. In particular, the filament geometry, appropriate for integration into textiles, is analyzed. Piezoelectric filaments producing electrical signals under bending or traction loads, thus acting as mechanical sensors, have been produced and tested, and are presented in this paper.

Key Words : Piezoelectric, PVDF, Multi-layered fibres, E-textiles

1. Introduction

In recent years, large efforts have been developed for the incorporation of systems and devices in textile products [1,2]. The main difficulties of integrating electronic products into textile materials result from the separate processing conditions and requirements for the textile and the device. Ideally, new fibres with increased functionality, such as sensing and actuating performance, should be used, being them a more significant part or even the complete solution for a given application.

There are several approaches for the production of textile products with transducing capabilities. One of the most interesting ones, from the industrialization point of view, would be that the textile material itself shows this functionality. This integration can occur at the level of the fibre, of the yarns or of the fabric and can be based on piezoelectric polymers.

2. Piezoelectric polymers and filaments

Poly(vinylidene fluoride), PVDF, is a widely studied material due to its piezoelectric properties, including in the context of integration into textiles. These properties can be used in applications such as sensor and actuator devices. The electroactive properties depend on the degree of crystallinity, structure and orientation of the crystalline fraction of the polymer, which in turn depend on the processing conditions [3].

PVDF presents at least 4 crystalline phases, the non-polar α-phase being the one typically obtained by crystallization from the melt [3]. The β-phase is the most interesting from the point of view of electrical activity and is most often obtained by stretching α-PVDF between 80 ºC and 120 ºC using a stretch ratio (R) between 3 and 5 [4,5].

In order to optimize the piezoelectric response and, therefore, the transduction capabilities, the dipolar moments have to be further oriented by the application of an electric field, i.e. through a poling process. The simplest method is the electrode poling method, in which the material is subjected to fields higher than the coercive field, about 120 MV/m, or ideally subjecting it to fields of about 300 MV/m [6], depending on the poling temperature. After poling, the piezoelectric response is optimized, i.e., a potential will be produced upon mechanical excitation of the polymer, or a mechanical action is produced in the polymer when it is subjected to an electric field.

PVDF-based sensors are available on the market in the form of films. In this case, a thin PVDF layer is deposited with metallic electrode layers on both sides which serve as electrodes for signal

* Corresponding author: E-mail: helder@det.uminho.pt, Tel : +351967001699, Fax: +351253510293

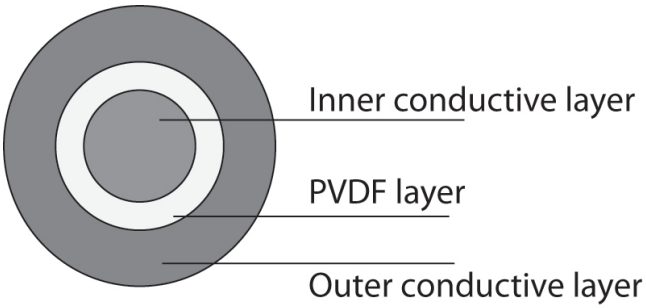

Fig.1 Structure of a coaxial piezoelectric filament.

acquisition and/or material stimulation.

Some research work has been focused on the development of PVDF sensors in the form of filaments. Walter *et al* [7, 8] have extensively studied the phase transitions in extruded PVDF monofilaments. A composite of simple PVDF filaments and epoxy resin with the filaments in a parallel arrangement was poled with a linear electric field in a direction perpendicular to the fibres. The composite was shown to exhibit piezoelectric activity.

From the point of view of textile use, a piezoelectric filament should ideally be arranged in a coaxial geometry, as shown in Fig. 1.

The production processes and poling methods for this arrangement have also been previously studied, in particular with respect to the study of the influence of the conductive layers on the piezoelectric properties of the PVDF [9-11]. Comprehensive work by Lund *et al* [10] and Ferreira *et al* [11] have shown for two-layered filaments that the electroactive phase content is not affected by the conductive inner core. The β-phase content depends only on the processing temperature and stretch ratio, as for the single PVDF filaments.

Sequential processing methods for piezoelectric cables have been described by Mazurek *et al* [12,13]. In such a process, the influence of cooling temperatures and the thermal impact of subsequent coating procedures are important to consider. Mazurek reports on an increase of 30 to 40 % of β-phase content for cooling temperatures of -30 ºC after stretching of the PVDF, when compared to cooling temperatures of 5 ºC. Also, a reduction between 20 to 50 % of the β-phase content was identified during the coating process necessary for the placement of the outer electrode, after the production of the inner layers.

In this work, multilayered fully polymer filaments incorporating electrically conductive layers used as electrodes, in a coaxial arrangement, are produced using a process based in conventional extrusion, more specifically using co-extrusion, that allow the filaments to be produced in a single step. This paper will focus on the production and properties of a two layer filament, composed of a conductive inner core and an outer PVDF layer. This kind of filamentary sensors can be used for applications such as health and security monitoring (breathing rate detection, movement and fall detection, human presence detection) when integrated into carpets, clothing or other textiles. Still another interesting possibility is the integration of these filaments into structures, mechanical parts or composite materials for structural or other types of physical monitoring and sensing. Finally, their use in energy-harvesting is also a possibility.

3. Experimental

3.1 Extrusion

A prototype monofilament extrusion line was used to produce the two-layered filament. The production steps are depicted in Fig. 2. As illustrated, the material leaves the extruder and is cooled in a water bath. Subsequently, the polymer enters a system of rolls (1) that imposes a certain linear velocity and travels through a heater followed by another system of rolls (2) that rotates at a higher speed. The combination of these two rolls systems, working at different speeds (V_1 and V_2) imposes a stretch ratio R to the filament quantified by

$$R = \frac{V_2}{V_1} \tag{1}$$

Stretching and heating the material at a controlled ratio and temperature are critical for achieving the required α- to β-phase transformation that should take place in the PVDF layer.

A modular die for co-extrusion of filaments with up to 4 different layers was designed and produced. In a first phase, it was used to

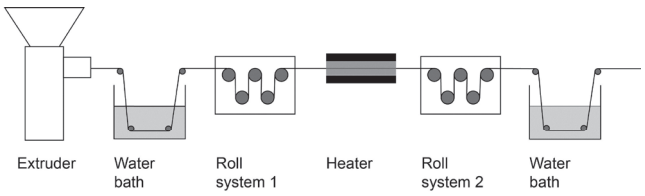

Fig.2 Production steps of two-layered coaxial piezoelectric filament.

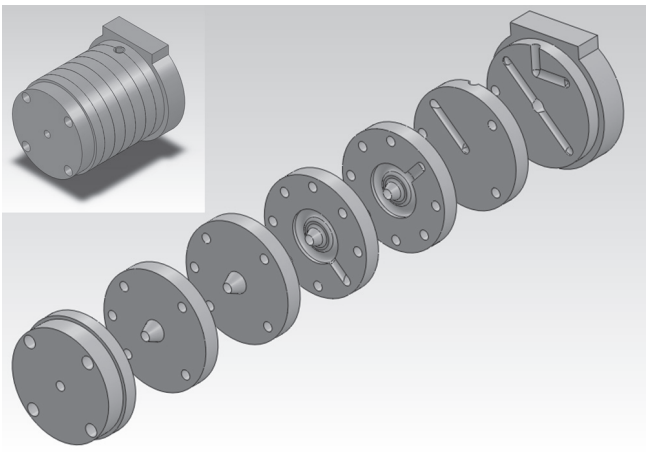

Fig.3 Construction of the extrusion die.

Table 1 Conditions for production of the filament.

Extrusion temperature (at die)- PVDF	235 ºC
Extrusion temperature (at die)- conductive PP	255 ºC
Extrusion speed	0.8 m/min
Stretch ratio	4
Water bath temperature	20 ºC
Heater temperature	180 ºC

produce two-layer filaments, with an inner conductive core and an outer PVDF layer. Fig. 3 shows the construction of the extrusion die.

The materials used were Solvay Solef Ta-1010 PVDF and Premix 1396 conductive PP, respectively, for the piezoelectric (outer) and conductive (inner) layers. Experimental tests allowed identifying the optimal conditions considering process stability, filament quality, maximum stretch ratio and electrical response. Table I shows the optimized extrusion process parameters.

Although the drawing temperature of 180 ºC is higher than the effective suggested drawing temperatures (80 to 120 ºC), it should be noted that unlike in a static drawing process, in the present case the filament drawing is obtained during production in dynamic conditions, in which the filament travels through the heater at a relatively high speed, not allowing the filament to stay in the heater for more than about two seconds. In this way, due to the poor thermal conductivity of the polymer, the filament does not reach the heater temperature. To assess the actual content of electroactive phase material, the β-phase content was determined, as described in the next section.

3.2 Determination of β-phase content of the samples

Fourier transformed infrared spectroscopy (FTIR) tests were performed in order to evaluate the β-phase content of the samples. Measurements were carried out with a Perkin-Elmer Spectrum 100 in ATR mode at room temperature.

Infrared absorption bands at 763 and 840 cm^{-1}, specific of the α- and β-phases [14], respectively, and a procedure similar to the one presented in [15] were used to quantify the amount of β-phase, which is given by

$$F(\beta) = \frac{X_\beta}{X_\alpha + X_\beta} = \frac{A_\beta}{(K_\beta TK_\alpha)A_\alpha + A_\beta} = \frac{A_\beta}{1.26A_\alpha + A_\beta} \quad (2)$$

where A_α and A_β are the absorbances at 763 and 840 cm^{-1}, corresponding to the α-and β-phase material; K_α and K_β are the absorption coefficients at the respective wave numbers, and X_α and X_β represent the degree of crystallinity of each phase. The value employed for K is 7.7×10^4 and 6.1×10^4 cm^2/mol for α- and β-phase, respectively [15].

3.3 Poling

The extruded filaments were cut into 10 cm long segments. The preparation was finished by creating an outer electrode using silver conductive ink and exposing the inner conductive layer. The two layers were then connected directly to a high-voltage source and the voltage was stepped up, seeking to maximize the electrical field applied (Figure 4). The voltage source's protection automatically stopped the voltage increase when current increased, which resulted either from material breakdown or localized defects. During the poling tests, voltages of about 9 kV were reached, which, considering the filament geometry, result in electric fields between 90 and 180 MV/m in the PVDF layer.

The samples were poled at 80 ºC during 20 minutes and cooled down to room temperature under the applied field, with the whole process taking 30 minutes.

3.4 Mechanical evaluation

For evaluation of the mechanical behavior of the filaments, three

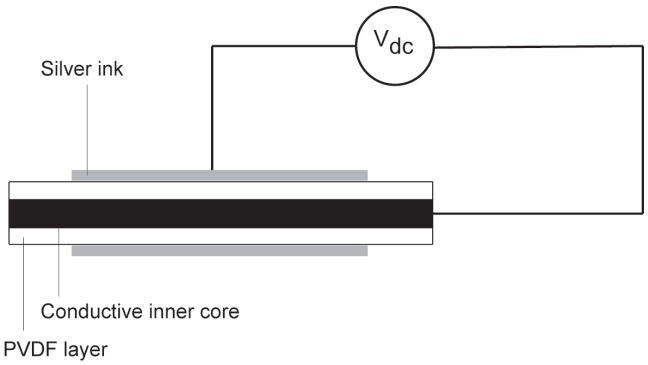

Fig.4 Connection for poling of the filament.

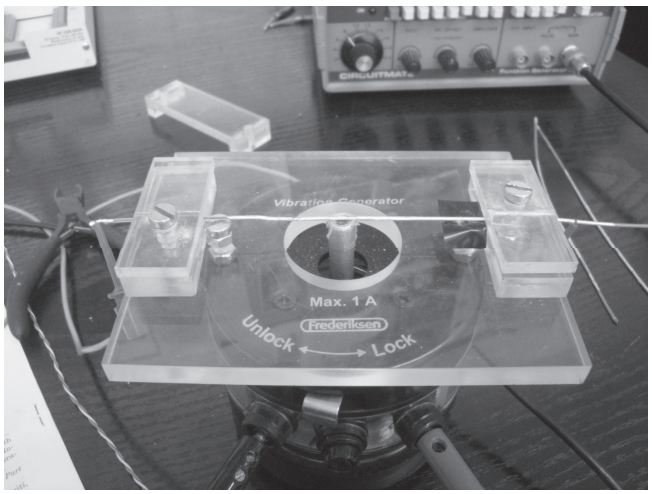

Fig.5 Electromechanical testing set-up based on a vibration generator.

filament samples were stretched in a universal testing machine (Shimadzu AG-IS 500 N) at a speed of 10 mm/min, until rupture, with an initial distance between grips of 35 mm.

3.5 Electrical evaluation

Two different experimental set-ups were used to test the electromechanical response of the produced filaments.

First, the filament was attached to a vibration generator (Figure 5) through a set of acrylic parts constructed for this purpose.

The vibration generator was fed with a 0.5 Hz square wave which produced an oscillating movement of the generator's axis with an amplitude of ~ 3 mm, and thus promoting bending deformation to the filament.

Second, the filaments were fixed to the grips of a universal testing machine, working in the tensile mode, and submitted to 20 loading-unloading cycles with 1 % extension at a speed of 100 mm/min. The distance between grips was 45 mm and a pre-tension of 5 N was applied to the filament.

3.6 Signal conditioning and acquisition

The filaments were connected to a custom-built charge amplifier, which is a specific circuit for this type of sensor (Figure 6). Piezoelectric sensors generate electrical potential upon force variations, but the charge unbalance involved in this process is very small and is quickly dissipated in a conventional amplifier. Therefore, static forces do not produce any signal. Using a charge amplifier, or charge-to-voltage converter, the signal is picked up and held in the capacitor present in the amplifier's feedback loop. To avoid saturation of the amplifier, a feedback resistor has to be used, and thus the capacitor discharges through the feedback resistor. The discharge time to 36.8 % of charge, known as the *time constant*, can be varied by adjusting the component values, and is given by:

$$T = R_f C_f \tag{3}$$

where

T : Capacitor discharge time constant [s]
R_f : Feedback resistor value [Ω]
C_f : Feedback capacitor value [F]

A piezoelectric sensor coupled to a charge amplifier can thus be dimensioned to perform measurements of low-frequency signals, although it is not able to measure purely static signals [16].

The capacitor value plays another important role: the amplifier gain is inversely proportional to this value:

$$G = \frac{1}{C_f} \tag{4}$$

where

G : Charge amplifier gain [V/C]

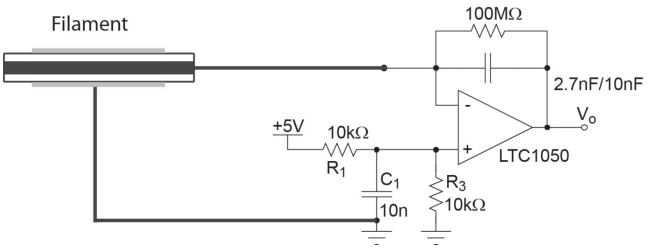

Fig. 6 Filament connection and signal conditioning via a charge amplifier.

Due to the configuration of the amplifier, the output signal is inverted: a negative voltage variation will be produced upon a positive charge variation produced by the sensor [16].

Equation (5) expresses the relation between electrical charge, capacity and voltage in a capacitor.

$$V = \frac{Q}{C} \tag{5}$$

with

V : Voltage [V]
Q : Electrical charge [C]
C : Capacity [F]

In fact, the voltage at the amplifier's output is the voltage at the feedback capacitor; this voltage is produced by the electrical charge moved by the sensor into the capacitor upon mechanical excitation.

The output signal of the amplifier was connected to a National Instruments NI-6259 data acquisition board and custom-developed software based on Labview was used for signal acquisition, display and storage. The amplifier is supplied directly by the 5 V single-supply of the data acquisition board and is provided with a 2.5 V offset to allow symmetrical signals varying around the offset.

The acquired signals showed to be affected by some 50 Hz-noise and its harmonics, which blurred the signals of smaller amplitude. Correct grounding and shielding of the conditioning electronics provided a significant reduction of this noise. A Butterworth 10th-order bandstop filter with a stopband between 45 and 55 Hz was implemented in the software and in this configuration even the smallest signals could be depicted.

4. Results and Discussion

4.1 Extrusion

Fig. 7 shows a cross-section and Fig. 8 a longitudinal cut of the two-layer co-extruded PVDF filament with conductive inner core.

It is observed that the shape of the layers is not fully axisymmetric, which is to be ascribed to the lack of optimization of the extrusion die used to produce the filaments. The modular nature of the die, which requires fine interplay between the different

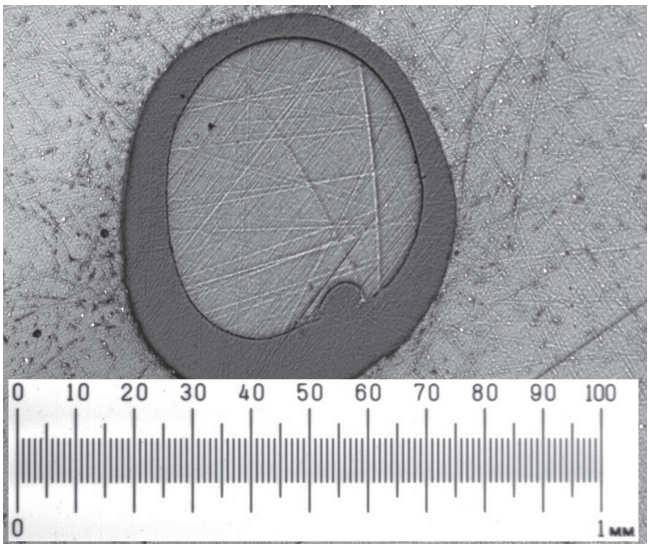

Fig. 7 Cross-section image of the filament: the inner layer is composed of the electrically conductive material and the external one of PVDF.

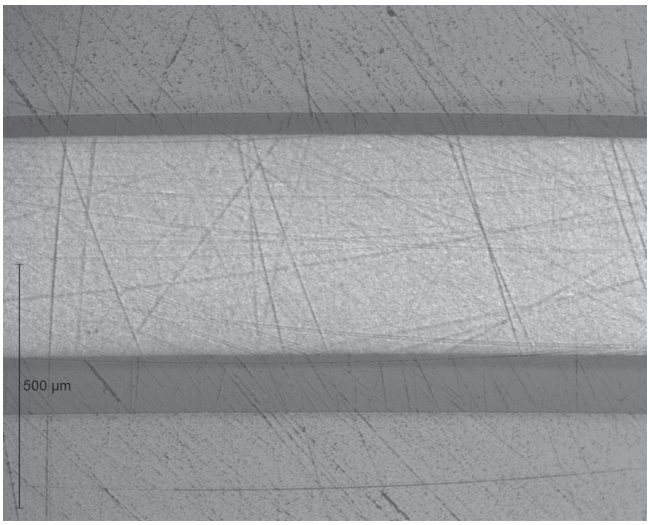

Fig.8 Longitudinal cut of the filament.

modules, the inexistence of a tuning mechanism and the complex rheological behavior of the materials employed, hinders an accurate process control and results in the asymmetric layer distribution obtained for the filament geometry. Nevertheless, it was possible to obtain continuous layers of the different materials that comprise the filament, which assures electrical conductivity in the inner layer and pickup of the electric signals in the piezoelectric layer.

A more even geometry of the filament would allow improvement in several aspects, among them the optimization of the poling procedure as, for example, the maximum electric field that can be applied is imposed by the thinnest points of the PVDF layer. However, an on-line tunable tool, required to handle different materials, layer thickness distribution and processing conditions, would have a prohibitive cost, not adequate for this phase of the investigation (proof of concept).

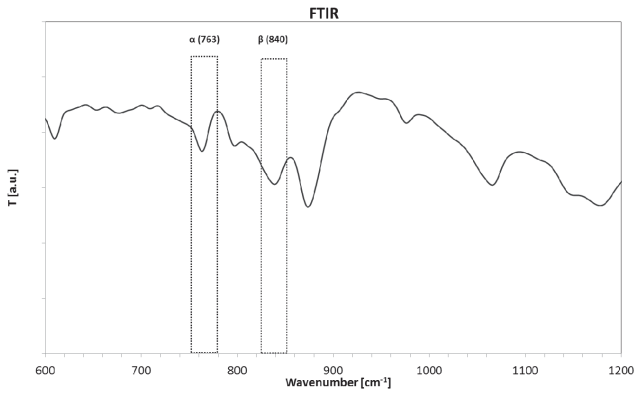

Fig.9 FTIR spectrum of the extruded samples.

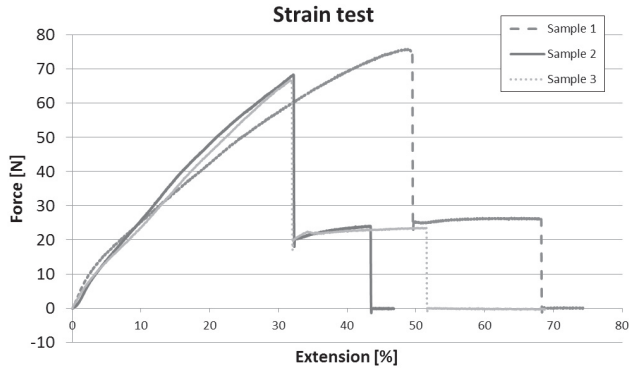

Fig.10 Strain test on three filament samples.

4.2 ß-phase content

Fig. 9 shows the FTIR spectrum obtained for the characterized filaments.

The calculation of ß-phase content according to the previously described method yields a result of 38 % of material in ß-phase. This is a relatively low value, considering that in previous experiments extruding simple PVDF filament contents of 70 to 80 % had been achieved. Still, this percentage of ß-phase material is sufficient for the filament to exhibit piezoelectric response, as will be presented in Section 4.4.

4.3 Mechanical test

Fig. 10 shows the results of the tensile test. It can be observed that the two layers of the filament break at different times. Simultaneous measurement of electrical resistance of the inner layer showed, as expected, that the PVDF layer is the last layer to fail.

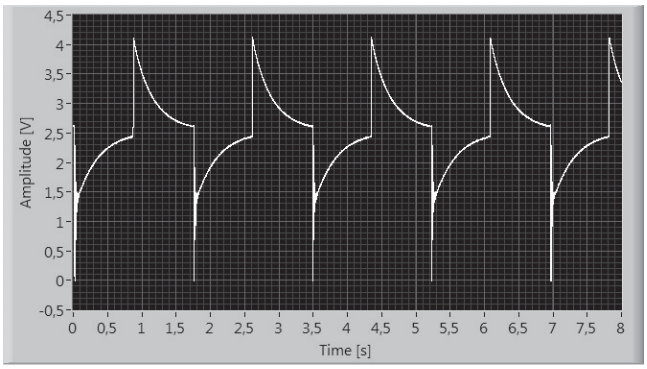

Fig. 11 Electric signal produced by mechanical excitation through the universal testing machine.

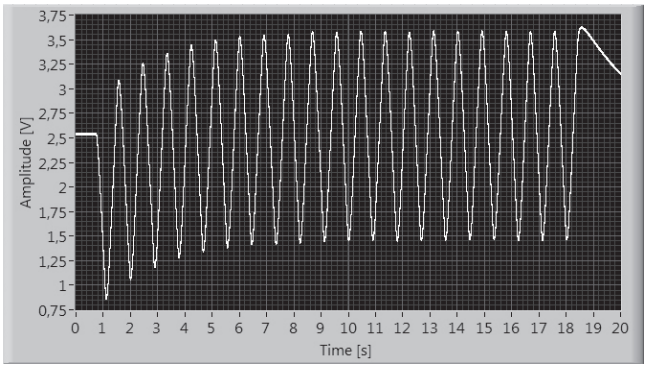

Fig. 13 Electric signal produced by traction through the universal testing machine.

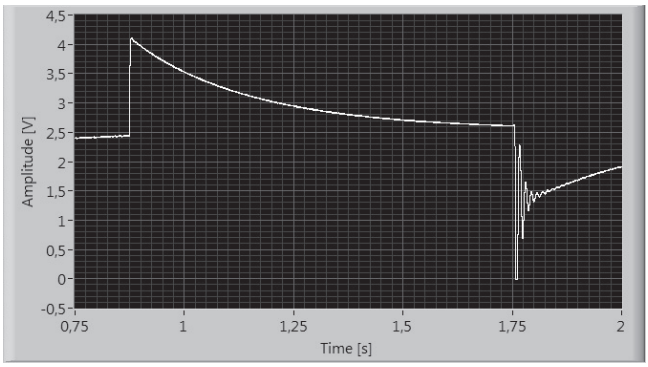

Fig. 12 Signal detail showing oscilation of filament when hit by the vibration generator's shaft.

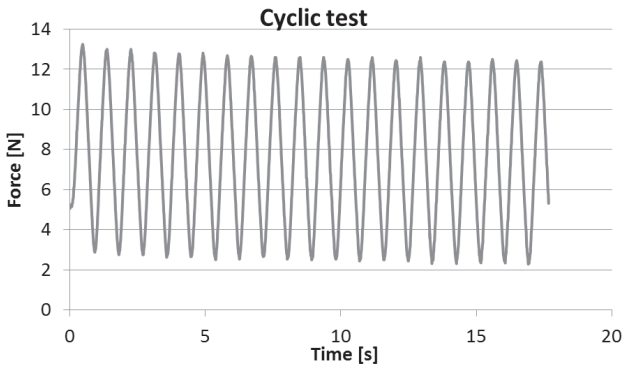

Fig. 14 Force measured by the universal testing machine during the cyclic test.

4.4 Electrical test and signals

Fig. 11 shows the signals resulting from the excitation of the filament with the vibration generator.

The response is typical for a piezoelectric sensor coupled to a charge amplifier, as explained in Section 3.3. For the current case, the calculation of the time constant of the charge amplifier, considering the values of C_f = 2.7 nF and R_f = 100 MΩ, yields t=0.27 s, which is in accordance with the observed signals.

The detail image presented in Fig. 12 shows how the generated signal can depict the oscillation which is produced when the vibration generator's shaft hits the filament. This gives a first indication of good performance in measuring dynamic signals at high frequency, as usual with piezoelectric sensors.

The amplitude of the measured signal is still roughly within the limits of the amplifier (0 to 5 V), but for the cyclic tensile test, the amplifier gain has to be reduced to avoid saturation of the amplifier. For this purpose, the amplifier's feedback capacitor was changed from a 2.7 nF to a 10 nF capacitor. Thus, the output voltage is reduced by a factor of 3.7 and the time constant increased by the same factor.

The traction applied by the universal testing machine produced the signal shown in Fig. 13. Fig. 14 shows the force applied to the filament, as measured by the testing machine.

It can be observed that the signal produced by the filament follows the variation of the imposed force. Considering the inverting action of the charge amplifier, the output is inverted relative to the applied force variation. Also, a drift of the output signal can be observed. This is mainly due to the nature of the force variation applied to the filament, which is not symmetric above zero because of the pre-tension applied – it has thus a static component. As described before, the piezoelectric measurement system responds to static values by eliminating them over time, with an associated time constant. A slight drift in the force values (Fig. 14) is added to this effect.

The amplitude of the electrical signal at cycle 11 is 2.1 V, corresponding to a force range of 9.5 N. For these values, the sensitivity of the sensor is computed as follows:

The charge injected into the capacitor for a force range of 9.5 N is

$$Q = V \cdot C = 2.1 \cdot 10 \cdot 10^{-9} = 21nC \qquad (6)$$

Thus, the sensitivity of the sensor can be calculated as

$$S = \frac{Q}{F} = \frac{21 \cdot 10^{-9}C}{9.5N} = 2.21\frac{nC}{N} \qquad (7)$$

For comparison purposes, a sensor based on commercial PVDF film (metallized film sheet from Measurement Specialties, 28 μm thickness) with approximately the same volume of PVDF was prepared. The cross-sectional area of the PVDF layer was measured and the approximate volume of the tested filament was computed. For the same volume, a strip of the PVDF film with dimensions 38 mm x 4 mm was prepared The testing machine was set to produce the same cyclic extension of 1 % in the longer direction of the strip and the electrical output of this sensor was measured using the same charge amplifier. The signal produced by this sensor was much higher and a feedback capacitor of 22 nF had to be used to lower the amplifier gain and avoid saturation. In this configuration, the measurement system produced 4.3 V for a force variation of 3.0 N. Repeating the calculation of equations 6 and 7, the output of the film-based sensor results as 31.5 nC/N, which is an order of magnitude higher than that produced by the filament.

There are several factors that should be considered to explain the low sensitivity of the filament sensor when compared to the film. In the first place, the ß-phase content of 38% found in the filament is quite low. Second, poling fields achieved in this experiment are also low. Although they exceed the coercive field, which is between 50 and 120 MV/m for PVDF, optimum performance of the piezoelectric material requires a poling field in excess of 300 MV/m [17]. An increase of the poling field may be achieved with a more even geometry of the filament, allowing increasing the poling voltage, or by reducing the PVDF layer thickness.

A third factor is the adhesion between the inner conductive layer and the PVDF layer. It has been observed that the contact of the conductive layer and the PVDF layer is not always optimal. This leads to internal losses inside of the filament, which also contribute to the decreased sensitivity.

5. Concluding remarks

A proof-of-concept has been given for a co-extruded filament sensor, which produces an electric signal when stimulated by traction, bending or other mechanical action.

Conditions for extrusion and drawing of the filament, in order to provide the electroactive properties of the filament, have been identified. The electroactive phase content of the filament has been measured using FTIR and was found to be of 38 %, a low value, but sufficient for the production of significant piezoelectric response.

The filament has been tested under bending and extension stress and its functionality as a sensor has been demonstrated. As a traction sensor, a sensitivity of 2.2 nC/N has been measured. A sensor of approximately equal volume of PVDF based on a commercial PVDF film provided 31.5 nC/N. Despite the low value obtained, the produced filament sensor exhibits enough sensitivity to provide quality signals without a particular amplifier design effort. A further optimization of the extrusion process can improve the sensitivity and geometry of the sensor, whose sensing capabilities and accuracy are just now starting to be explored.

The next step is the production of three-layered filaments, in which the outer electrode is produced during the extrusion process itself, by co-extruding a third electrically conductive layer and thus eliminating the step of creating the outer electrode. The optimization of the process and the reduction of the filament's cross-sectional dimensions can then lead to the mass-production of low-cost electroactive materials with full textile integration for various applications.

Acknowledgements

This work was supported by FEDER through the COMPETE Program and by the Portuguese Foundation for Science and Technology (FCT) in the framework of the Strategic Project PEst-C/FIS/UI607/20112011, PEst-C/CTM/LA0025/2011 (Strategic Project - LA 25 - 2011-2012) and PEst-C/CTM/UI0264/2011, and projects PTDC/CTM/108801/2008, PTDC/CTM/69316/2006 and PTDC/CTM-NAN/112574/2009 and former Plurianual programmes. They also wish to thank the IN2TEC initiative of the School of Engineering/University of Minho which supported some initial work on piezoelectric filaments and the COST actions MP1003 (The 'European Scientific Network for Artificial Muscles' (ESNAM)), and MP0902 (Composites of Inorganic Nanotubes and Polymers (COINAPO)).

References

[1] Meoli D, May-Plumlee T (2002) Journal of Textile and Apparel, Technology and Management, **2**, 1-12

[2] Edmison J, Jones M, Nakad Z, Martin T (2002) Proceedings Sixth International Symposium on Wearable Computers (ISWC 2002), 41-48

[3] Lovinger J (1982) "Developments in crystalline polymers", Elsevier Applied Science, London

[4] Gomes J, Nunes JS, Sencadas V, Lanceros-Mendez S (2010) Smart Materials and Structures, **19**, 065010

[5] Sencadas V, Jr. RG, Lanceros-Mendez S(2009) Journal of Macromolecular Science, Part B: Physics, **48**, 514-525

[6] Dickens B, Balizer E, DeReggi AS, Roth SC(1992) J Appl Phys, **72**, 4258-4264

[7] Walter S, Steinmann W, Schütte J, Seide G, Gries T, Roth G, Wierach P, Sinapius M (2011) Materials Technology: Advanced Performance Materials, **26**, 140-145

[8] Steinmann W, Walter S, Seide G, Gries T, Roth G, Schubnell M (2011) Structure, properties, and phase transitions of melt-spun poly(vinylidene fluoride) fibres, Journal of Applied Polymer Science, vol. 120, **1**, 21-35

[9] Martins RS, Silva MP, Gonçalves R, Rocha JG, Nóbrega JM, Carvalho H, Souto AP, Lanceros-Mendez S (2012) Proceedings of the TRS2012 The 41st Textile Research Symposium, 222-227

[10] Lund A, Hagström B (2011) Journal of Applied Polymer Science, **120**, 1080-1089

[11] Ferreira A, Costa P, Carvalho H, Nobrega, JM, Sencadas, V, Lanceros-Mendez S (2011) Journal of Polymer Research, **18**, 1653-1658

[12] Mazurek B, Rozecki S, Kowalzcyk T (2000) The 6th International Conference on Properties and Applications of Dielelectric Materials, 1041- 1044

[13] Mazurek B, Różecki S, Kowalczyk D, Janiczek T (2001) Journal of Electrostatics, **51**, 180-185

[14] Mano JF, Costa AM, and Schmidt VH (2001) Journal of Macromolecular Science, **40**, 517–527

[15] Martins P, Lopes AC, Lanceros-Mendez S (2014) Progress in Polymer Science, **39**, 683-706

[16] Gautschi G (2002) "Piezoelectric Sensorics: Force, Strain, Pressure, Acceleration and Acoustic Emission Sensors, Materials and Amplifiers", Springer-Verlag, Berlin

[17] Dickens B, Balizer E, DeReggi AS, Roth SC (1992) J Appl Phys, **72**, 4258-4264